Inorg. Chem. **2005**, *44*, 7109–7121

Modulation of the Ring Size and Nuclearity of Metallamacrocycles via the Steric Effect of Ligands: Preparation and Characterization of 18-Membered Hexanuclear, 24-Membered Octanuclear, and 30-Membered Decanuclear Manganese Metalladiazamacrocycles with α- and β-Branched *N*-Acylsalicylhydrazides

Rohith P. John,[†] Kyungjae Lee,[†] Beom Jin Kim,[‡] Byoung Jin Suh,[‡] Hackjune Rhee,[†] and Myoung Soo Lah*,[†]

Department of Chemistry and Applied Chemistry, College of Science and Technology, Hanyang University, Ansan, Kyunggi-Do 426-791, Korea, and Department of Physics, Catholic University of Korea, Puchon, 420-473, Korea

Received June 2, 2005

Hexanuclear, octanuclear, and decanuclear manganese metalladiazamacrocycles have been prepared by reacting a series of pentadentate ligands, *N*-acylsalicylhydrazides (*N*-(3-methylbutanoyl)salicylhydrazide ($H_3$3-mbshz), *N*-(phenylacetyl)salicylhydrazide (H_3pashz), *N*-(3,3-dimethylbutanoyl)salicylhydrazide ($H_3$3-dmbshz), *N*-(2-methylpropanoyl)salicylhydrazide ($H_3$2-mpshz), *N*-((*R,S*)-2-methylbutanoyl)salicylhydrazide (H_3*RS*-2-mbshz), *N*-((*S*)-2-methylbutanoyl)salicylhydrazide (H_3*S*-2-mbshz), and *N*-(2,2-dimethylpropanoyl)salicylhydrazide ($H_3$2-dmpshz)), with manganese(II) acetate tetrahydrate. The self-assembled, supramolecular complexes assume a nearly planar cyclic structure with an $-(Mn-N-N)_n$ backbone and measure ∼2.1, ∼2.3, and ∼2.6 nm in outer diameters for $n = 6$, 8, and 10, respectively. The chiralities of the manganese centers on the metalladiazamacrocycle occur in alternating ···ΛΔΛΔ··· configurations. While β-branched *N*-acylsalicylhydrazides ($H_3$3-mbshz, H_3pashz, $H_3$3-dmbshz) with a sterically flexible Cα methylene group yield 18-membered hexanuclear manganese metalladiazamacrocycles of S_6 point group symmetry, α-branched *N*-acylsalicylhydrazides lead to 24-membered octanuclear manganese metalladiazamacrocycles or 30-membered decanuclear manganese metalladiazamacrocycles depending on the size of the *N*-acyl substituents. The α-branched $H_3$2-mpshz ligand with the sterically least demanding isopropyl tail at the *N*-acyl position yields a 24-membered octanuclear manganese metalladiazamacrocycle of S_8 point group symmetry, but other α-branched *N*-acylsalicylhydrazides such as H_3*RS*-2-mbshz, H_3*S*-2-mbshz, and $H_3$2-dmpshz lead to 30-membered decanuclear manganese metalladiazamacrocycles of S_{10} point group symmetry. The magnetic properties of the metalladiazamacrocycles are characterized by a weak antiferromagnetic exchange interaction, with $J_{eff} = -8.5$ to -3.8 K between the Mn^{3+} ion spins with $S = 2$ in the cyclic system.

Introduction

A variety of high nuclearity metal−organic assemblies such as self-assembled polynuclear structures,[1] metallamacrocycles,[2] and single molecular magnets[3] have gained importance in recent years due to their interesting molecular architecture[4] and magnetic properties.[5] Metallamacrocycles and metallacages were found to form interesting host−guest systems with different metal ions of varying coordination and symmetry.[6] They were also used as secondary building units for the construction of metal−organic framework

* To whom correspondence should be addressed. E-mail: mslah@hanyang.ac.kr. Fax: 82 31 407 3863. Tel: 82 31 400 5496.
[†] Hanyang University.
[‡] Catholic University.

(1) (a) Wang, X.; Vittal, J. J. *Inorg. Chem.* **2003**, *42*, 5135. (b) Thompson, L. K.; Matthews, C. J.; Zhao, L.; Xu, Z.; Miller, D. O.; Wilson, C.; Leech, M. A.; Howard, J. A. K.; Heath, S. A.; Wittaker, A. G.; Winpenny, R. E. P. *J. Solid State Chem.* **2001**, *159*, 308. (c) Zhao, L.; Xu, Z.; Thompson, L. K.; Miller, D. O. *Polyhedron* **2001**, *20*, 1359. (d) Baxter, P. N. W.; Khoury, R. G.; Lehn, J.-M.; Baum, G.; Fenske, D. *Chem.—Eur. J.* **2000**, *6*, 4141. (e) Belletti, D.; Graif, C.; Massera, C.; Pattacini, R.; Predieri, G.; Tiripicchio, A. *Inorg. Chim. Acta* **2003**, *356*, 187. (f) Kitagawa, S.; Kitaura, R.; Noro, S.-I. *Angew. Chem., Int. Ed.* **2004**, *43*, 2334.

10.1021/ic050891h CCC: $30.25
Published on Web 08/27/2005

structures.[7] Metal ions such as Ga, Co, Fe, and Mn that can easily form stable octahedral coordination are found to yield hexanuclear metallamacrocycles with trianionic pentadentate ligands *N*-acylsalicylhydrazides (H_3xshz).[8,9] Manganese and iron have received special attention due to their ease of formation of metallamacrocycles and interesting magnetic properties.[10,11] Controlling the ring size and nuclearity of metallamacrocycles and their properties has recently become of interest. The use of *N*-acylsalicylhydrazides with linear aliphatic tails was found to form a metal−diaza backbone, $-(M-N-N)_n$, where $n = 6$, and to result in isostructural hexanuclear manganese metalladiazamacrocycles.[12] The alternation of the Λ and Δ configurations of the metal centers can be regarded as the reason for the cycle formation, where the configurations of the metal centers are derived from propeller binding modes (five- and six-membered chelating rings using a tridentic *N*-acylhydraziminolate group in the meridional mode and five-membered chelating ring using a bidentic hydrazidate group) of the pentadentate ligand.[8,9,13] It is understood that the nature of *N*-acyl groups can influence the size and nuclearity of the macrocycle formed. Of late, the use of a sterically bulkier phenyl group at the *N*-acyl position of the salicylhydrazide was found to yield a decanuclear metalladiazamacrocycle with manganese and iron ions,[11] while the presence of the isopropyl tail was found to give an octanuclear iron metalladiazamacrocycle.[10] A dodecanuclear manganese metalladiazamacrocycle has also been synthesized by employing the ligand, *trans*-2-pentenoyl salicylhydrazide, with a geometrical constraint at the *N*-terminal group.[13] As part of our efforts to understand the steric effect of *N*-acyl side chains on the size and nuclearity of metalladiazamacrocycles, and to develop a better understanding of the magnetic behavior of metalladiazamacrocycles, we report here the synthesis and characterization of hexanuclear, octanuclear, and decanuclear manganese metalladiazamacrocycles of a series of pentadentate ligands with systematically controlled β-branched *N*-acylsalicylhydrazides (viz., $H_3$3-mbshz, H_3pashz, $H_3$3-dmbshz) and α-branched *N*-acylsalicylhydrazides ($H_3$2-mpshz, H_3*RS*-2-mbshz, H_3*S*-2-mbshz, $H_3$2-dmpshz) (Chart 1).

Experimental Section

Materials. The following materials were used as received with no further purification: salicylhydrazide, dimethyl sulfoxide (dmso), dimethyl sulfoxide-d_6, acetone-d_6, 3-methylbutyryl chloride, phenylacetyl chloride, 3,3-dimethylbutyryl chloride, 3,3-dimethylbutanoic acid, 2-methylpropionyl chloride, 2-methylpropanoic acid, 2-methylbutyryl chloride, (*S*)-(+)-2-methylbutyric anhydride, 2,2-dimethylpropionyl chloride, triethylamine, and pyridine (py) from Aldrich, Inc.; manganese(II) acetate tetrahydrate from Yakuri; dimethyl sulfoxide (dmso), dimethylformamide (dmf), dimethylacetamide (dma), chloroform, and hexane from Junsei Chemical Co., Ltd.

(2) (a) Moon, M.; Kim, I.; Lah, M. S. *Inorg. Chem.* **2000**, *39*, 2710. (b) Horikoshi, R.; Mochida, T.; Kurihara, M.; Mikuria, M. *Cryst. Growth Des.* **2005**, *5*, 243. (c) Campbell, K.; Johnson, C. A., II; McDonald, R.; Ferguson, M. J.; Haley, M. M.; Tykwinski, R. R. *Angew. Chem., Int. Ed*. **2004**, *43*, 5967. (d) Shan, N.; Vickers, S. J.; Adams, H.; Ward, M. D.; Thomas, J. A. *Angew. Chem., Int. Ed*. **2004**, *43*, 3938. (e) Panda, S.; Singh, H. B.; Butcher, R. J. *Chem. Commun*. **2004**, 322. (f) Severin, K. *Coord. Chem. Rev.* **2003**, *245*, 3. (g) Galindo, M. A.; Galli, S.; Navarro, J. A. R.; Romero, M. A. *Dalton Trans.* **2004**, 2780. (h) Stott, T. L.; Wolf, M. O.; Lam, A. *Dalton Trans.* **2005**, 652. (i) Ohi, H.; Tachi, Y.; Itoh, S. *Inorg. Chem.* **2004**, *43*, 4561. (j) Masar, M. S., III; Mirkin, C. A.; Stern, C. L.; Zakharov, L. N.; Rheingold, A. L. *Inorg. Chem.* **2004**, *43*, 4693. (k) Brasey, T.; Scopelliti, R.; Severin, K. *Inorg. Chem.* **2005**, *44*, 160. (l) Helliwell, M.; Smith, A. A.; Teat, S. J.; Winpenny, R. E. P. *Inorg. Chim. Acta* **2003**, *354*, 49. (m) Thuéry, P.; Villiers, C.; Jaud, J. L.; Ephritikhine, M.; Masci, B. *J. Am. Chem. Soc*. **2004**, *126*, 6838. (n) Kuehl, C. J.; Huang, S. D.; Stang, P. J. *J. Am. Chem. Soc.* **2001**, *123*, 9634. (o) Weng, Z.; Teo, S.; Koh, L. L.; Hor, T. S. A. *Organometallics* **2004**, *23*, 3603.

(3) (a) Philippov, A. V.; Platonov, V. V.; Selemir, V. D.; Tatsenko, O. M.; Zvezdin, A. K.; Canesch, A. *Condens. Matter* **2002**, 1. (b) Tsai, H.-L.; Chen, D. M.; Yang, C. I.; Jwo, T.-Y.; Wur, C.-S.; Lee, G.-H.; Wang, Y. *Inorg. Chem. Commun*. **2001**, 511. (c) Milios, C. J.; Raptopoulou, C. P.; Terzis, A.; Lloret, F.; Vicente, R.; Perlepes, S. P.; Escuer, A. *Angew. Chem., Int. Ed.* **2004**, *43*, 210. (d) Murugesu, M.; Wernsdorfer, W.; Abboud, K. A.; Christou, G. *Angew. Chem., Int. Ed.* **2005**, *44*, 892. (e) Jones, L. F.; Batsanov, A.; Brechin, E. K.; Collison, D.; Helliwell, M.; Mallah, T.; McInnes, E. J. L.; Pilikgos, S. *Angew. Chem. Int. Ed.* **2002**, *41*, 4318. (f) Tasiopoulos, A. J.; Vinslava, A.; Wernsdorfer, W.; Abboud, K. A.; Christou, G. *Angew. Chem. Int. Ed.* **2004**, *43*, 2117. (g) Costes, J.-P.; Clemente-Juan, J. M.; Dahan, F.; Milon, J. *Inorg. Chem*. **2004**, *43*, 8200. (h) Ferbinteanu, M.; Miyasaka, H.; Wernsdorfer, W.; Nakata, K.; Sugiura, K.-i.; Yamashita, M.; Coulon, C.; Clérac, R. *J. Am. Chem. Soc*. **2005**, *127*, 3090.

(4) (a) Rojo, J.; Romero-Salguero, F. J.; Uppadine, L. H.; Lehn, J.-M. *Angew. Chem., Int. Ed.* **2004**, *43*, 3644. (b) Hapler, S. R.; Cohen, S. M. *Angew. Chem. Int. Ed.* **2004**, *43*, 2385. (c) Kumazawa, K.; Biradha, K.; Kusukawa, T.; Okano, T.; Fujita, M. *Angew. Chem., Int. Ed*. **2003**, *42*, 3909. (d) Pereira, C. L. M.; Pedroso, E. F.; Stumpf, H. O.; Novak, M. A.; Ricard, L.; Garcia, R. R.; Riviere, E.; Journaux, Y. *Angew. Chem., Int. Ed.* **2004**, *43*, 956. (e) He, Z.; He, C.; Wang, Z.-M.; Gao, E.-Q.; Liu, Y.; Yan, C.-H. *Dalton Trans.* **2004**, 502.

(5) (a) Stemmler, A. J.; Kampf, J. W.; Kirk, M. L.; Atasi, B. H.; Pecoraro, V. L. *Inorg. Chem.* **1999**, *38*, 2807. (b) Costes, J.-P.; Dahan, F.; Donnadieu, B.; Douton, M.-J. R.; Garcia, M.-I. F.; Bousseksou, A.; Tuchagues, J.-P. *Inorg. Chem*. **2004**, *43*, 2736. (c) Caneschi, A.; Cornia, A.; Fabretti, A. C.; Gatteschi, D. *Angew. Chem., Int. Ed.* **1999**, *38*, 1295. (d) Abu-Nawwas, A.-A. H.; Cano, J.; Christian, P.; Mallah, T.; Rajaraman, G.; Teat, S. J.; Winpenny, R. E. P.; Yukawa, Y. *Chem. Commun.* **2004**, 314. (e) Samara, C. D.; Psomas, G.; Iordanidis, L.; Tangoulis, V.; Kessissoglou, D. P. *Chem.*−Eur. J. **2001**, *7*, 5041. (f) Abbati, G. L.; Cornia, A.; Caneschi, A.; Fabretti, A. C.; Mortalo, C. *Inorg. Chem.* **2004**, *43*, 4540. (g) Koizumi, S.; Nihei, M.; Nakano, M.; Oshio, H. *Inorg. Chem.* **2005**, *44*, 1208.

(6) (a) Bark, T.; Duggeli, M.; Evans, H. S.; von Zelewsky, A. *Angew. Chem., Int. Ed.* **2001**, *40*, 2848. (b) Kumazawa, K.; Biradha, K.; Kusukawa, T.; Okano, T.; Fujita, M. *Angew. Chem., Int. Ed*. **2003**, *42*, 3909. (c) Beatty, A. M. *Coord. Chem. Rev*. **2003**, *246*, 131. (d) Cutland, A. D.; Malkani, R. G.; Kampf, J. W.; Pecoraro, V. L. *Angew. Chem., Int. Ed*. **2000**, *39*, 2689. (e) Aluarez, C. S.; Bond, A. D.; Harron, E. A.; Layfield, R. A.; McAllister, J. A.; Pask, C. M.; Rawson, J. M.; Wright, D. S. *Organometallics* **2001**, *20*, 4135.

(7) (a) Moon, D.; Lah, M. S. *Inorg. Chem.* **2005**, *44*, 1934. (b) Moon, D.; Song, J.; Kim, B. J.; Suh, B. J.; Lah, M. S. *Inorg. Chem.* **2004**, *43*, 8230. (c) Shin, D. M.; Lee, I. S.; Chung, Y. K.; Lah, M. S. *Inorg. Chem*. **2003**, *42*, 5459. (d) Su, C.-Y.; Yang, X.-P.; Kang, B. S.; Mak, T. C. W. *Angew. Chem., Int. Ed.* **2001**, *40*, 1726.

(8) (a) Kwak, B.; Rhee, H.; Park, S.; Lah, M. S. *Inorg. Chem.* **1998**, *37*, 3599. (b) Kim, I.; Kwak, B.; Lah, M. S. *Inorg. Chim. Acta* **2001**, *317*, 12. (c) Song, J.; Moon, D.; Lah, M. S. *Bull. Korean Chem. Soc*. **2002**, *23*, 708.

(9) (a) Kwak, B.; Rhee, H.; Lah, M. S. *Polyhedron* **2000**, *19*, 1985. (b) Lin, S.; Liu, S.-X.; Huang, J.-Q.; Lin, C.-C. *J. Chem. Soc., Dalton Trans.* **2002**, 1595. (c) Kim, I.; Kwak, B.; Lah, M. S. *Inorg. Chim. Acta* **2001**, *317*, 12. (d) Lin, S.; Liu, S.-X.; Lin, B.-Z. *Inorg. Chim. Acta* **2002**, *328*, 69.

(10) Lin, S.; Liu, S.-X.; Chen, Z.; Lin, B.-Z.; Gao, S. *Inorg. Chem.* **2004**, *43*, 2222.

(11) Liu, S.-X.; Lin, S.; Lin, B.-Z.; Lin, C.-C.; Huang, J.-Q. *Angew. Chem., Int. Ed.* **2001**, *40*, 1084.

(12) We proposed earlier a more specific terminology for this class of compounds as "metalladiazamacrocycles" because a metal and two nitrogens constitute the repeating unit in the macrocyclic ring system.[13] These complexes could also be termed metallamacrocycles as a more general terminology for macrocycles containing metal ions as ring constituents.

(13) John, R. P.; Lee, K.; Lah, M. S. *Chem. Commun.* **2004**, 2660.

Chart 1. Schematic Drawing of Ligands with Different *N*-Acyl Substituents

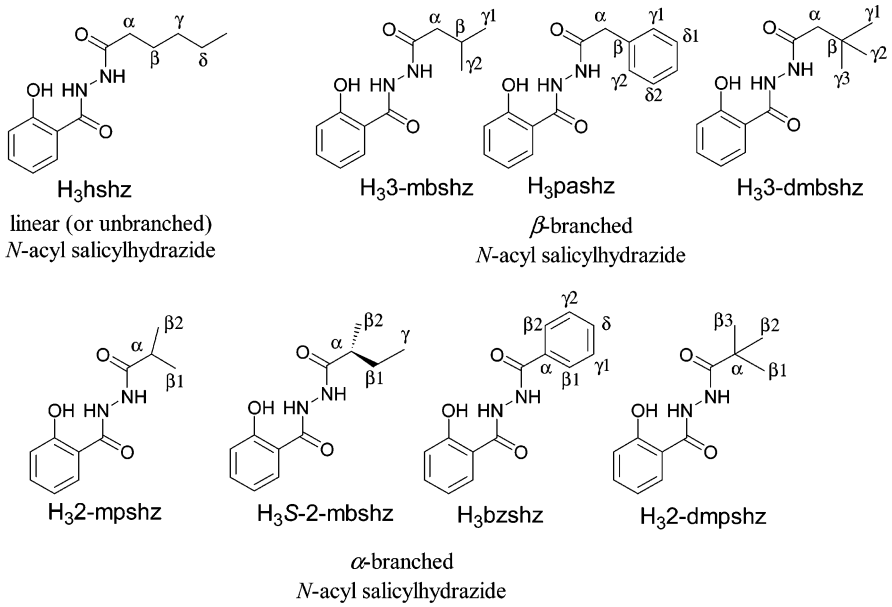

Instrumentation. Elemental analyses (C, H, and N) were performed at the Korea Research Institute of Chemical Technology and the Elemental Analysis Laboratory of the Korean Basic Science Institute. Infrared spectra were recorded as KBr pellets in the range 4000−600 cm^{-1} on a BioRad FT-IR spectrometer. ESI mass spectra were obtained using an HP Agilent 1100 MSD mass spectrometer. NMR spectra were obtained using a Varian-300 spectrometer. Temperature-dependent magnetic susceptibility measurements were carried out on powdered samples between 2 and 300 K using a Quantum Design MPMS-7XL SQUID magnetometer. Field-cooled magnetization data were collected at $H = 1000$ Oe. The diamagnetic correction for each complex was calculated using Pascal's constants.

Preparation of Ligands. *N*-(3-Methylbutanoyl)salicylhydrazide ($H_3$3-mbshz). 3-Methylbutyryl chloride (1.24 mL, 10.0 mmol) was added to a solution of chloroform (90 mL) containing water (0.18 mL, 10.0 mmol) and triethylamine (2.85 mL, 20.0 mmol) at 0 °C. The reaction mixture was slowly warmed to ambient temperature. Then a further amount of 3-methylbutyryl chloride (1.24 mL, 10.0 mmol) was added to the mixture and stirred for a further 2 h. At the completion of the above reaction, salicylhydrazide (1.43 g, 9.2 mmol) was added to the reaction mixture. The resulting reaction mixture was stirred at ambient temperature for 1 day. The clear solution was reduced to half its volume and then diluted with hexane (40 mL), kept under refrigeration overnight, filtered, and washed with ether, and rinsed with water (30 mL × 3) followed by ether. It was then dried in vacuo over P_2O_5 (1.73 g, 79.7% yield). Mp: 170−171 °C. IR (KBr pellet, cm^{-1}): 3235 (s), 2964 (m), 2952 (m), 2904 (w), 2871 (w), 1674 (m), 1606 (s), 1569 (s), 1486 (s), 1453 (m), 1429 (w), 1359 (m), 1313 (m), 1234 (m), 1210 (m), 1158 (m), 1127 (w), 1100 (w), 1042 (w), 1018 (w), 880 (m), 859 (w), 823 (w), 750 (m), 705 (m), 668 (m), 592 (w). ^{1}H NMR (300 MHz, acetone-d_6, ppm): δ 11.88 (s (br), 1H), 9.97 (s (br), 1H) (both amide NH's), 9.21 (s, 1H, phenolic OH), 7.87 (d, 1H, Ar), 7.44 (t, 1H, Ar), 6.86−6.94 (m, 2H, Ar), 2.06−2.19 (t and m, 3H, $-CH_{2-}$ and $-CH-$), 0.99 (d, 6H, $-CH(CH_3)_2$). ^{13}C NMR (75.5 MHz, acetone-d_6, ppm): δ 170.12 (C_8), 166.76 (C_7), 158.97 (C_1), 133.93 (C_5), 128.17 (C_3), 118.89 (C_4), 117.21 (C_2), 114.38 (C_6), 42.39 (C_9), 25.59 (C_{10}), 22.36 (C_{11}). ESI mass spectrum: m/z of $[C_{12}H_{16}N_2O_3 + H]^+$, 237.2. Anal. Calcd for $C_{12}H_{16}N_2O_3$ (M = 236.27): C, 61.00; H, 6.83; N, 11.86. Found: C, 61.21; H, 7.04; N, 11.87.

***N*-(Phenylacetyl)salicylhydrazide (H_3pashz).** The ligand was prepared in a manner analogous to that used for *N*-3-methylbutanoylsalicylhydrazide. Phenylacetyl chloride was used in place of 3-methylbutyryl chloride. The product formed was filtered out, washed successively with water and ether, and dried in vacuo over P_2O_5 (1.95 g, 78.4% yield). Mp: 227−229 °C. IR (KBr pellet, cm^{-1}): 3182 (s), 3142 (s), 3027 (m), 2848 (w), 2690 (w), 2549 (w), 1687 (w), 1606 (s), 1574 (s), 1504 (m), 1487 (s), 1452 (m), 1419 (m), 1355 (m), 1308 (m), 1233 (m), 1185 (w), 1157 (w), 1100 (w), 1074 (w), 1041 (w), 1008 (w), 905 (w), 781 (w), 764 (w), 751 (m), 728 (m), 704 (m). ^{1}H NMR (300 MHz, dmso-d_6, ppm): δ 11.84 (s (br), 1H), 10.61 (s (br), 1H) (both amide NH's), 10.49 (s, 1H, phenolic OH), 7.85 (d, 1H, Ar), 7.42 (t, 1H, Ar), 7.31, 7.33 (d, s, 4H, Bz), 7.20−7.26 (m, 3H, Bz), 6.88−6.95 (m, 2H, Ar), 3.56 (s, 2H, $-CH_{2-}$). ^{13}C NMR (75.5 MHz, dmso-d_6, ppm): δ 168.76 (C_8), 166.55 (C_7), 158.84 (C_1), 135.51 (C_{10}), 134.09 (C_5), 129.10 (C_{11}), 128.46 (C_{12}), 128.30 (C_3), 126.61 (C_{13}), 119.12 (C_4), 117.31 (C_2), 114.64 (C_6), 40.24 (C_9). ESI mass spectrum: m/z of $[C_{15}H_{14}N_2O_3 + H]^+$, 271.3. Anal. Calcd for $C_{15}H_{14}N_2O_3$ (M = 270.29): C, 66.66; H, 5.22; N, 10.36. Found: C, 67.39; H, 5.36; N, 10.46.

***N*-(3,3-Dimethylbutanoyl)salicylhydrazide ($H_3$3-dmbshz).** An aliquot of 1.24 mL (10.0 mmol) of 3,3-dimethylbutyryl chloride was added dropwise to a stirred solution of chloroform (50 mL) containing 1.30 mL (10.0 mmol) of 3,3-dimethylbutanoic acid and 1.47 mL (10.5 mmol) of triethylamine at 0 °C. Stirring was continued for another 30 min, and the solution was brought gradually to ambient temperature. An amount of 1.42 g (9.5 mmol) of salicylhydrazide was then added to the mixture, with stirring being continued for another 1 h. About 20 mL of hexane was added to the resulting solution, which was kept under refrigeration overnight. The product formed was filtered out, washed successively with water and ether, and dried in vacuo over P_2O_5 (1.69 g, 71.1% yield). Mp: 229−231 °C. IR (KBr pellet, cm^{-1}): 3283 (m), 3185 (m), 2960 (m), 2867 (w), 1668 (w), 1631 (m), 1603 (s), 1571 (s), 1511 (m), 1487 (s), 1455 (m), 1366 (m), 1313 (w), 1241 (m), 1204 (w), 1160 (w), 1104 (w), 1043 (w), 1015 (w), 894 (w), 880 (w), 858 (w), 828 (w), 779 (w), 749 (m). ^{1}H NMR (300 MHz, dmso-d_6, ppm): δ 11.95 (s (br), 1H), 10.52 (s (br), 1H) (both amide NH's), 10.04 (s, 1H, phenolic OH), 7.88 (d, 1H, Ar), 7.42 (t, 1H, Ar), 6.89−6.95 (m, 2H, Ar), 2.09 (s, 2H, $-CH_{2-}$), 1.03 (s, 9H,

−C(CH_3)$_3$). ^{13}C NMR (75.5 MHz, dmso-d_6, ppm): δ 169.16 (C_8), 166.70 (C_7), 158.97 (C_1), 133.91 (C_5), 128.20 (C_3), 118.88 (C_4), 117.22 (C_2), 114.41 (C_6), 46.46 (C_9), 30.64 (C_{10}), 29.70 (C_{11}). ESI mass spectrum: m/z of $[C_{13}H_{18}N_2O_3 + H]^+$, 251.3. Anal. Calcd for $C_{13}H_{18}N_2O_3$ (M = 250.30): C, 63.15; H, 7.25; N, 11.33. Found: C, 62.38; H, 7.13; N, 11.19.

***N*-(2-Methylpropanoyl)salicylhydrazide ($H_3$2-mpshz).** An aliquot of 2.16 mL (2.0 mmol) of 2-methylpropionyl chloride was added to 20 mL of chloroform containing 3.09 mL (2.2 mmol) of triethylamine and 1.88 mL (2.0 mmol) of 2-methylpropanoic acid at 0 °C while stirring. The solution was slowly warmed to room temperature, and 3.07 g (1.98 mmol) of salicylhydrazide was added in small portions. Stirring was continued for about 1 h, and upon completion of the reaction, it was diluted with 20 mL of hexane and left overnight to precipitate. The white product formed was filtered out and washed with small portions of cold chloroform and then with water and ether, followed by drying in vacuo over P_2O_5 (3.04 g, 69.1% yield). Mp: 156−158 °C. IR (KBr pellet, cm^{-1}): 3332 (s), 3309 (s), 3067 (m), 2973 (m), 2877 (w), 1668 (s), 1639 (s), 1608 (s), 1564 (m), 1484 (s), 1458 (m), 1386 (m), 1377 (m) 1314 (w), 1240 (m), 1212 (m), 1106 (m), 1034 (w), 957 (w), 907 (w), 869 (w), 793 (w), 751 (m), 668 (w). ^{1}H NMR (300 MHz, dmso-d_6, ppm): δ 11.88 (s (br), 1H), 10.52 (s (br), 1H) (both amide NH's), 10.07 (s, 1H, phenolic OH), 7.88 (d, 1H, Ar), 7.43 (t, 1H, Ar), 6.89−6.97 (m, 2H, Ar), 2.54 (m, 1H, −CH−), 1.09 (d, 6H, −(CH_3)$_2$). ^{13}C NMR (75.5 MHz, dmso-d_6, ppm): δ 174.91 (C_8), 166.90 (C_7), 159.09 (C_1), 134.03 (C_5), 128.21 (C_3), 118.96 (C_4), 117.28 (C_2), 114.54 (C_6), 32.06 (C_9), 20.02 (C_{10}). ESI mass spectrum: m/z of $[C_{11}H_{14}N_2O_3 + H]^+$, 223.3. Anal. Calcd for $C_{11}H_{14}N_2O_3$ (M = 222.24): C, 59.45; H, 6.35; N, 12.60. Found: C, 59.27; H, 6.29; N, 12.73.

***N*-((*R*,*S*)-2-Methylbutanoyl)salicylhydrazide (H_3*RS*-2-mbshz).** 2-Methylbutyryl chloride (1.03 mL, 8.29 mmol) was added to a solution of chloroform (30 mL) containing water (0.15 mL, 8.29 mmol) and triethylamine (2.3 mL, 16.58 mmol) at 0 °C. The reaction mixture was slowly warmed to ambient temperature. More 2-methylbutyryl chloride (1.03 mL, 8.29 mmol) was added to the mixture. Then, salicylhydrazide (1.05 g, 6.91 mmol) was added to the reaction mixture. The resulting reaction mixture was stirred at ambient temperature for 1 day. The white suspension was diluted with hexane (70 mL), filtered, and rinsed with water (30 mL × 3) and hexane (30 mL × 5), before being dried over P_2O_5 in vacuo (1.24 g, 76.0% yield). Mp: 147−149 °C. IR (KBr pellet, cm^{-1}): 3336 (m), 3245 (s), 3040 (m), 2971 (s), 2937 (m), 2879 (m), 2724 (w), 1683 (m), 1640 (s), 1608 (s), 1523 (s), 1490 (s), 1458 (s), 1373 (m), 1315 (m), 1243 (m), 1214 (m), 1160 (w), 1145 (w), 1103 (w), 1038 (w), 973 (w), 940 (w), 904 (w), 867 (w), 826 (w), 753 (m). ^{1}H NMR (300 MHz, dmso-d_6, ppm): δ 11.98, 10.54, 10.11 (s, s, s, 3H, amides and phenolic OH), 7.88 (dd, 1H, phenyl), 7.44 (td, 1H, phenyl), 6.90−6.97 (m, 2H, phenyl), 2.32 (m, −CH−), 1.61−1.51, 1.42−1.33 (m, m, 2H, −CH_2CH$_3$), 1.06 (d, 3H, −CHCH_3), 0.89 (t, 3H, −CH$_2$CH_3). ^{13}C NMR (75.5 MHz, dmso-d_6, ppm): δ 174.42 (C_8), 167.07 (C_7), 159.22 (C_1), 134.09 (C_5), 128.26 (C_3), 119.02 (C_4), 117.35 (C_2), 114.46 (C_6), 39.36 (C_9), 26.74 (C_{10}), 17.48 (C_{12}), 11.78 (C_{11}). ESI mass spectrum: m/z of $[C_{12}H_{16}N_2O_3 + H]^+$, 237.2. Anal. Calcd for $C_{12}H_{16}N_2O_3$ (M = 236.27): C, 61.00; H, 6.83; N, 11.86. Found: C, 60.75; H, 6.73; N, 11.79.

***N*-((*S*)-2-Methylbutanoyl)salicylhydrazide (H_3*S*-2-mbshz).** Salicylhydrazide (0.304 g, 2.00 mmol) was added to (*S*)-(+)-2-methylbutyric anhydride (2 mL) at ambient temperature. A white suspension was immediately obtained. The suspension was filtered and rinsed with hexane and water. It was then dried in vacuo over P_2O_5 (0.33 g, 70% yield). Mp: 148−150 °C. IR (KBr pellet, cm^{-1}): 3333 (m), 3245 (s), 3039 (m), 2970 (s), 2936 (m), 2878 (m), 2723 (w), 1683 (m), 1640 (s), 1607 (s), 1523 (s), 1490 (s), 1458 (s), 1374 (m), 1314 (m), 1241 (m), 1216 (m), 1162 (w), 1146 (w), 1104 (w), 1038 (w), 973 (w), 940 (w), 902 (w), 826 (w), 753 (m). ^{1}H NMR (300 MHz, dmso-d_6, ppm): δ 11.94, 10.51, 10.08 (s (br), s (br), s, 3H, amides and phenolic OH), 7.85 (dd, 1H, phenyl), 7.41 (td, 1H, phenyl), 6.88−6.94 (m, 2H, phenyl), 2.31 (m, 1H, −CHCH$_3$), 1.60−1.48, 1.43−1.32 (m, m, 2H, −CH_2CH$_3$), 1.05 (d, 3H, −CHCH_3), 0.89 (t, 3H, −CH$_2$CH_3). ^{13}C NMR (75.5 MHz, dmso-d_6, ppm): δ 174.20 (C_8), 166.86 (C_7), 159.03 (C_1), 133.93 (C_5), 128.11 (C_3), 118.88 (C_4), 117.22 (C_2), 114.33 (C_6), 39.37 (C_9), 26.78 (C_{10}), 17.54 (C_{12}), 11.84 (C_{11}). ESI mass spectrum: m/z of $[C_{12}H_{16}N_2O_3 + H]^+$, 237.2. Anal. Calcd for $C_{12}H_{16}N_2O_3$ (M = 236.27): C, 61.00; H, 6.83; N, 11.86. Found: C, 60.89; H, 6.60; N, 11.81.

***N*-(2,2-Dimethylpropanoyl)salicylhydrazide ($H_3$2-dmpshz).** The ligand was prepared in a manner analogous to that used for *N*-((*R*,*S*)-2-methylbutanoyl)salicylhydrazide, except that 2,2-dimethylpropionyl chloride was used instead of 2-methylbutyryl chloride. The product was washed successively with hexane, water, and ether and then dried over P_2O_5 in vacuo (1.29 g, 78.7% yield). Mp: 163−164 °C. IR (KBr pellet, cm^{-1}): 3411 (m), 3382 (m), 3286 (s), 3228 (s), 3024 (m), 2972 (s), 2874 (m), 1672 (m), 1649 (s), 1631 (m), 1598 (s), 1530 (m), 1492 (s), 1447 (w), 1369 (m), 1360 (m), 1347 (m), 1316 (w), 1294 (w), 1261 (m), 1230 (w), 1214 (s), 1168 (m), 1145 (w), 1121 (w), 1038 (w), 941 (w), 931 (w), 892 (w), 860 (w), 828 (w), 816 (w), 778 (w), 753 (s), 699 (w), 668 (w). ^{1}H NMR (300 MHz, dmso-d_6, ppm): δ 12.04, 10.43, 9.70 (s (br), s (br), s, 3H, amides and phenolic OH), 7.88 (d, 1H, phenyl), 7.44 (t, 1H, phenyl), 6.89−6.96 (m, 2H, phenyl), 1.19 (s, 9H, −C(CH_3)$_3$). ^{13}C NMR (75.5 MHz, dmso-d_6, ppm): δ 176.68 (C_8), 167.85 (C_7), 159.55 (C_1), 134.13 (C_5), 128.04 (C_3), 118.97 (C_4), 117.42 (C_2), 114.33 (C_6), 37.64 (C_9), 27.22 (C_{10}). ESI mass spectrum: m/z of $[C_{12}H_{16}N_2O_3 + H]^+$, 237.2. Anal. Calcd for $C_{12}H_{16}N_2O_3$ (M = 236.27): C, 61.00; H, 6.83; N, 11.86. Found: C, 60.95; H, 6.59; N, 11.84.

Synthesis of Metalladiazamacrocycles. [Mn(3-mbshz)(dmso)]$_6$ (1). An amount of 23.6 mg (0.10 mmol) of *N*-(3-methylbutanoyl)-salicylhydrazide was dissolved in 15 mL of dmso, and 24.5 mg (0.10 mmol) of manganese(II) acetate tetrahydrate was added to the solution without stirring. The solution was allowed to stand for 12 days, whereupon dark brown crystals of X-ray quality were obtained (24.5 mg, 66.9% yield). IR bands (KBr, cm^{-1}): 3437 (br), 3068 (w), 2997 (w), 2955 (s), 2927 (m), 2870 (m), 1706 (w), 1602 (s), 1566 (s), 1511 (s), 1466 (m), 1443 (w), 1432 (w), 1405 (s), 1366 (s), 1322 (s), 1274 (w), 1254 (w), 1247 (m), 1222 (w), 1170 (w), 1149 (m), 1110 (m), 1037 (m), 1016 (s), 953 (m), 909 (m), 883 (w), 856 (w), 826 (w), 754 (s), 695 (w), 684 (s), 659 (w), 642 (m), 595 (m). Anal. Calcd for $[Mn_6(3\text{-mbshz})_6(dmso)_5(H_2O)]$ ($Mn_6C_{82}H_{110}N_{12}O_{24}S_5$) ($M$ = 2137.77): C, 46.07; H, 5.19; N, 7.86; S, 7.50. Found: C, 46.47; H, 5.24; N, 7.74; S, 7.92.

[Mn(pashz)(dmso)]$_6$ (2). Complex **2** was prepared in a manner analogous to that of **1**, [Mn(3-mbshz)(dmso)]$_6$. An amount of 27.0 mg (0.10 mmol) of *N*-(phenylacetyl)salicylhydrazide in 15 mL of dmso and 24.5 mg (0.10 mmol) of manganese(II) acetate tetrahydrate were used for complexation. Dark brown crystals of X-ray quality were obtained after 8 days (25.3 mg, 63.2% yield). IR bands (KBr, cm^{-1}): 3440 (br), 3062 (w), 2918 (w), 1602 (s), 1561 (s), 1507 (s), 1466 (w), 1453 (m), 1443 (m), 1424 (m), 1406 (s), 1357 (m), 1324 (m), 1255 (m), 1247 (m), 1148 (m), 1109 (w), 1015 (m), 952 (m), 900 (w), 859 (m), 785 (w), 755 (m), 726 (m), 695 (m), 687 (m), 639 (w), 594 (w), 472 (w). Anal. Calcd for

$[Mn(pashz)(dmso)]_6$ ($Mn_6C_{102}H_{102}N_{12}O_{24}S_6$) ($M$ = 2401.99): C, 51.00; H, 4.28; N, 7.00; S, 8.01. Found: C, 50.95; H, 4.33; N, 6.72; S, 7.65.

$[Mn(3\text{-}dmbshz)(dmso)]_6$ (3). Complex **3** was prepared in a manner analogous to that of **1**, $[Mn(3\text{-}mbshz)(dmso)]_6$. An amount of 25.0 mg (0.10 mmol) of *N*-(3,3-dimethylbutanoyl)salicylhydrazide in 15 mL of dmso and 24.5 mg (0.10 mmol) of manganese(II) acetate tetrahydrate were used. Good quality crystals were obtained over a period of 10 days (23.0 mg, 60.5% yield). IR (KBr, cm^{-1}): 3442 (br), 2951 (m), 2870 (m), 1602 (s), 1567 (s), 1512 (s), 1466 (w), 1444 (m), 1424 (m), 1406 (s), 1361 (m), 1324 (m), 1274 (m), 1254 (m), 1246 (m), 1145 (m), 1109 (w), 1036 (m), 1019 (m), 952 (m), 903 (w), 888 (w), 859 (m), 787 (w), 754 (m), 726 (m), 696 (m), 683 (m), 641 (w), 547 (w). Anal. Calcd for $[Mn_6(3\text{-}dmbshz)_6(dmso)_5(H_2O)]\cdot H_2O$ ($Mn_6C_{88}H_{124}N_{12}O_{25}S_5$) ($M$ = 2239.95): C, 47.19; H, 5.58; N, 7.50. Found: C, 46.97; H, 5.27; N, 7.54.

$[Mn(2\text{-}mpshz)(dmso)]_8$ (4). An amount of 88.9 mg (0.40 mmol) of *N*-(2-methylpropanoyl)salicylhydrazide was dissolved in a mixture of 8 mL of dmso and 2 mL of methanol, and 100.0 mg (0.40 mmol) of manganese(II) acetate tetrahydrate was added to it. Compound **4** was obtained as fine microcrystalline needles on standing for 8 days (135.0 mg, 94.0% yield). IR (KBr, cm^{-1}): 3439 (br), 2975 (m), 1602 (s), 1566 (s), 1507 (s), 1469 (w), 1443 (m), 1407 (m), 1349 (m), 1324 (m), 1247 (m), 1148 (w), 1110 (w), 1083 (w), 1016 (m), 954 (w), 906 (w), 855 (w), 758 (m), 687 (m), 669 (m), 649 (w), 604 (w). Anal. Calcd for $[Mn_8(2\text{-}mpshz)_8(dmso)_8]\cdot 6dmso\cdot 5H_2O$ ($Mn_8C_{116}H_{182}N_{16}O_{43}S_{14}$) ($M$ = 3377.15): C, 41.26; H, 5.43; N, 6.64; S, 13.29. Found: C, 41.12; H, 5.13; N, 6.99; S, 13.17. X-ray-quality crystals were obtained from a solution of *N*-(2-methylpropanoyl)salicylhydrazide (0.1 mmol) and manganese(II) acetate (0.1 mmol) in a mixture of dmso and methanol (12:3 mL) after a period of 15 days.

$[Mn(\mathit{RS}\text{-}2\text{-}mbshz)(dmf)]_{10}$ (5a). An amount of 23.6 mg (0.10 mmol) of *N*-((*R*,*S*)-2-methylbutanoyl)salicylhydrazide was dissolved in 20 mL of dmf, and 24.5 mg (0.10 mmol) of manganese(II) acetate tetrahydrate was added to the solution without stirring. The solution was allowed to stand for 10 days, whereupon dark brown crystals were obtained (25.6 mg, 70.9% yield). IR bands (KBr, cm^{-1}): 3434 (br), 2966 (m), 2934 (w), 2877 (w), 1656 (m), 1602 (s), 1567 (s), 1499 (s), 1467 (m), 1445 (s), 1409 (s), 1380 (m), 1353 (s), 1314 (m), 1243 (m), 1149 (w), 1110 (w), 903 (m), 859 (m), 808 (w), 756 (m), 696 (m), 649 (w), 603 (w). Anal. Calcd for $Mn_{10}(\mathit{RS}\text{-}2\text{-}mbshz)_{10}(dmf)(H_2O)_9$ ($Mn_{10}C_{123}H_{155}N_{21}O_{40}$) ($M$ = 3117.08): C, 47.40; H, 5.01; N, 9.44. Found: C, 47.81; H, 4.70; N, 9.47.

$[Mn(\mathit{S}\text{-}2\text{-}mbshz)(dmf)]_{10}$ (5b). Compound **5b** was prepared in a manner analogous to that of **5a**, $[Mn(\mathit{RS}\text{-}2\text{-}mbshz)(dmf)]_{10}$. An amount of 59.1 mg (0.25 mmol) of *N*-((*S*)-2-methylbutanoyl)-salicylhydrazide, and 61.3 mg (0.25 mmol) of manganese(II) acetate tetrahydrate were used (38.0 mg, 42.1% yield). IR bands (KBr, cm^{-1}): 3420 (br), 2966 (m), 2934 (w), 2877 (w), 1655 (m), 1602 (s), 1566 (s), 1498 (s), 1467 (m), 1446 (s), 1409 (s), 1379 (m), 1353 (s), 1315 (m), 1243 (m), 1149 (w), 1110 (w), 1036 (w), 904 (m), 860 (m), 808 (w), 755 (m), 696 (m), 651 (w), 606 (w). Anal. Calcd for $Mn_{10}(\mathit{S}\text{-}2\text{-}mbshz)_{10}(dmf)_3(H_2O)_7$ ($C_{129}H_{165}Mn_{10}N_{23}O_{40}$) ($M$ = 3227.24): C, 48.01; H, 5.15; N, 9.98. Found: C, 48.67; H, 4.78; N, 9.39.

$[Mn(2\text{-}dmpshz)(py)]_{10}$ (6). Compound **6** was prepared in a manner analogous to that of **5a**, $[Mn(\mathit{RS}\text{-}2\text{-}mbshz)(dmf)]_{10}$. An amount of 23.6 mg (0.10 mmol) of *N*-(2,2-dimethylpropanoyl)-salicylhydrazide in 20 mL of dma and py mixed solvent (3:1 ratio) and 24.51 mg (0.10 mmol) of manganese(II) acetate tetrahydrate were used (20.0 mg, 54.6% yield). IR bands (KBr, cm^{-1}): 3440 (br), 3067 (w), 2962 (m), 2931 (w), 2872 (w), 1602 (s), 1569 (s), 1503 (s), 1480 (s), 1446 (s), 1407 (s), 1397 (s), 1335 (s), 1324 (s), 1244 (m), 1224 (m), 1173 (w), 1148 (w), 1109 (w), 1069 (w), 1036 (m), 898 (m), 859 (m), 820 (w), 754 (m), 698 (s), 656 (w), 610 (w). Anal. Calcd for $Mn_{10}(2\text{-}dmpshz)_{10}(py)(H_2O)_9$ ($C_{125}H_{153}Mn_{10}N_{21}O_{39}$) ($M$ = 3123.09): C, 48.07; H, 4.94; N, 9.42. Found: C, 48.12; H, 5.00; N, 9.52.

Crystallographic Data Collections and Refinements of Structures. All crystals were coated in paratone oil, and preliminary examination and data collection were performed at −100 °C with Mo Kα radiation (λ = 0.710 73 Å) on a Bruker SMART CCD equipped with a graphite crystal, incident-beam monochromator. Cell constants and orientation matrixes for data collection were obtained from least-squares refinement with a set of 45 narrow-frame (0.3° in ω) scans. The SMART and SAINT software packages[14] were used for data collection and integration, respectively. Collected data were corrected for absorbance using SADABS[15] on the basis of Laue symmetry using equivalent reflections. All structures were solved by direct methods and refined by full-matrix least-squares calculations with the SHELXTL-PLUS software package (version 5.1).[16]

H_3pashz. All non-hydrogen atoms were refined anisotropically, and all hydrogen atoms were found from the difference Fourier map and refined isotropically.

$[Mn(3\text{-}mbshz)(dmso)]_6$ (1). All non-hydrogen atoms were refined anisotropically; hydrogen atoms were assigned isotropic displacement coefficients $U(H) = 1.2U(C)$ or $1.5U(C_{methyl})$, and their coordinates were allowed to ride on their respective atoms. The coordinated dmso molecule is statistically disordered, while an additional noncoordinated dmso site was found in the crystal lattice.

$[Mn(pashz)(dmso)]_6$ (2). All non-hydrogen atoms were refined anisotropically; hydrogen atoms were assigned isotropic displacement coefficients $U(H) = 1.2U(C)$ or $1.5U(C_{methyl})$, and their coordinates were allowed to ride on their respective atoms. A solvent dmso molecule was coordinated to the ring metal ion, while two free solvent dmso molecules were observed in the crystal lattice of **2**.

$[Mn(3\text{-}dmbshz)(dmso)]_6$ (3). All non-hydrogen atoms were refined anisotropically; hydrogen atoms were assigned isotropic displacement coefficients $U(H) = 1.2U(C)$ or $1.5U(C_{methyl})$, and their coordinates were allowed to ride on their respective atoms. A solvent dmso molecule was coordinated to the ring metal ion, and a free solvent dmso site was found to exist in the crystal lattice.

$[Mn(2\text{-}mpshz)(dmso)]_8$ (4). Non-hydrogen atoms with geometrical rigidity were refined anisotropically, but non-hydrogen atoms with geometrical flexibility were refined isotropically; hydrogen atoms attached to the nondisordered part were assigned isotropic displacement coefficients $U(H) = 1.2U(C)$ or $1.5U(C_{methyl})$, and their coordinates were allowed to ride on their respective atoms. A total of 16 dmso, 2 methanol, and 5 water solvent sites were found to exist in the crystal lattice. Several dmso molecules were statistically disordered, and one of them could be partially assigned.

$[Mn(\mathit{RS}\text{-}2\text{-}mbshz)(dmf)]_{10}$ (5a). All non-hydrogen atoms except some atoms of the solvent molecules were refined anisotropically; hydrogen atoms were assigned isotropic displacement coefficients

(14) *SMART and SAINT, Area Detector Software Package and SAX Area Detector Integration Program*; Bruker Analytical X-ray: Madison, WI, 1997.
(15) *SADABS, Area Detector Absorption Correction Program*; Bruker Analytical X-ray: Madison, WI, 1997.
(16) Sheldrick, G. M. *SHELXTL-PLUS, Crystal Structure Analysis Package*; Bruker Analytical X-ray: Madison, WI, 1997.

U(H) = 1.2U(C) or 1.5U(C_{methyl}), and their coordinates were allowed to ride on their respective atoms. One of the coordinate dmf molecules was statistically disordered. Three additional dmf solvent sites were observed. The solvent molecules behaved poorly, and the bond distances and angles of the solvent molecules were restrained to ideal geometry during the least-squares refinement.

[Mn(*S*-2-mbshz)(dmf)]$_{10}$ (5b). All non-hydrogen atoms except some atoms of the disordered side chains or solvent molecules were refined anisotropically; hydrogen atoms were assigned isotropic displacement coefficients U(H) = 1.2U(C) or 1.5U(C_{methyl}), and their coordinates were allowed to ride on their respective atoms. Enantiopure **5b** of pseudo-S_{10} symmetry is in a crystallographic inversion center, and this results in the disordering of the chiral *N*-(*S*)-2-methylbutanoyl side chains of the complex. An additional three dmf and one water sites were observed. The solvent molecules again behaved poorly, and the bond distances and angles of the solvent molecules were restrained to ideal geometry during the least-squares refinement.

[Mn(2-dmpshz)(py)]$_{10}$ (6). All non-hydrogen atoms except some atoms of the solvent molecules were refined anisotropically; hydrogen atoms were assigned isotropic displacement coefficients U(H) = 1.2U(C) or 1.5U(C_{methyl}), and their coordinates were allowed to ride on their respective atoms. Only pyridine molecules were coordinated to the ring metal ion. One of the coordinated pyridine molecules was disordered. Several dma, pyridine, and water sites were observed. The solvent molecules were restrained to ideal geometry during the least-squares refinement.

Summarized crystal data are given in Table 1.

Results and Discussion

Synthesis and Characterization. As mentioned in our previous reports,[7a,8,9a] we have employed the potential pentadentate ligand, *N*-acylsalicylhydrazide, as the backbone for the synthesis of metalladiazamacrocycles. The synthesis of the ligand involves reaction of an appropriate acid formed in situ (or added directly into the solution) with its corresponding acid chloride to form an acid anhydride, which then reacts with salicylhydrazide to give the corresponding *N*-acylsalicylhydrazide ligand. The general method for preparation of the complex involved dissolution of the respective ligand in solvents such as dmf/dma/dmso/py or a mixture of any of these and addition of manganese(II) acetate tetrahydrate in the solid form in a 1:1 ratio. Manganese(II) undergoes slow oxidation to manganese(III) in solution and binds with the triply deprotonated pentadentate *N*-acylsalicylhydrazide (H_3xshz) ligands (Scheme 1). As a consequence, the ligand is able to form neutral complexes with trivalent metal ions of octahedral geometry. Depending on the *N*-acyl side chains, hexanuclear, octanuclear, or decanuclear metallamacrocycles could be obtained. The ligands (H_3xshz) undergo deprotonation to form trianionic xshz^{3-} ions; the tridentic *N*-acylhydraziminolate group of the ligand binds to a manganese atom in the meridional mode, and the bidentic hydrazidate group of the adjacent ligand binds to the same manganese atom in a chiral propeller configuration. The sixth position of the metal center is satisfied by the solvent oxygen/nitrogen (O4/N3). The alternate occurrence of Λ and Δ configurations[8,9,13] at the metal centers closes the repeating metal−diaza backbone −(Mn−N−N)$_n$ into a ring system. The number of metal ions involved in the ring

Table 1. Crystal Data for H_3pashz and Complexes **1**−**4**, **5a**,**b**, and **6**[a]

param	H_3pashz	**1**	**2**	**3**	**4**	**5a**	**5b**	**6**
chem formula	$C_{15}H_{14}N_2O_3$	$C_{96}H_{150}Mn_6N_{12}O_{30}S_{12}$	$C_{110}H_{126}Mn_6N_{12}O_{28}S_{10}$	$C_{102}H_{162}Mn_6N_{12}O_{30}S_{12}$	$C_{242}H_{387}Mn_{16}N_{32}O_{87.50}S_{32}$	$C_{165}H_{235}Mn_{10}N_{35}O_{45}$	$C_{168}H_{246}Mn_{10}N_{36}O_{48}$	$C_{215}H_{253.50}Mn_{10}N_{40}O_{40.50}$
M	270.28	2666.64	2714.47	2750.80	7049.80	3978.28	4087.41	4595.48
cryst system	monoclinic	rhombohedral	triclinic	rhombohedral	triclinic	monoclinic	monoclinic	monoclinic
space group	$P2_1/n$	$R\bar{3}$	$P\bar{1}$	$R\bar{3}c$	$P\bar{1}$	$C2/c$	$C2/c$	$P2_1/n$
a/Å	5.2239(13)	18.1966(7)	14.517(2)	18.4008(16)	20.185(8)	39.044(3)	39.187(5)	21.430(14)
b/Å	10.145(3)	18.1966(7)	15.045(3)	18.4008(16)	23.590(10)	20.7050(17)	20.494(5)	25.110(15)
c/Å	25.113(6)	31.898(3)	15.957(3)	64.805(11)	36.387(15)	28.139(2)	28.283(5)	22.833(13)
α, β, γ/deg	$\alpha = \gamma = 90$, $\beta = 91.289(5)$	$\alpha = \beta = 90$, $\gamma = 120$	$\alpha = 62.116(3)$, $\beta = 81.716(3)$, $\gamma = 85.744(3)$	$\alpha = \beta = 90$, $\gamma = 120$	$\alpha = 91.366(8)$, $\beta = 100.792(9)$, $\gamma = 110.964(8)$	$\alpha = \gamma = 90$, $\beta = 118.231(2)$	$\alpha = \gamma = 90$, $\beta = 118.755(5)$	$\alpha = \gamma = 90$, $\beta = 108.593(16)$
V (Å^3)	1330.5(6)	9147.0(9)	3048.3(9)	19003(4)	15815(11)	20042(3)	19913(7)	11645(12)
Z	4	3	1	6	2	4	4	2
T/K	173(2)	173(2)	173(2)	173(2)	173(2)	173(2)	173(2)	173(2)
μ/mm^{-1}	0.096	0.883	0.851	0.852	0.909	0.686	0.694	0.600
R_{int}	0.0443	0.0192	0.0309	0.0310	0.0830	0.1375	0.1490	0.1456
tot. reflcns	8185	19 378	18 915	38 002	97 475	43 805	61 214	58 578
no. of indpt reflcns	3165	4952	13 691	5202	71 393	14 408	23 634	20 495
final R indices[b] $[I > 2\sigma(I)]$	R1 = 0.0481, wR2 = 0.0992,	R1 = 0.0497, wR2 = 0.1300	R1 = 0.0548, wR2 = 0.1160	R1 = 0.0444, wR2 = 0.1145	R1 = 0.1193, wR2 = 0.2598	R1 = 0.0821, wR2 = 0.1958	R1 = 0.1044, wR2 = 0.2527	R1 = 0.0915, wR2 = 0.2039
R indices (all data)	R1 = 0.1108, wR2 = 0.1241	R1 = 0.0568, wR2 = 0.1382	R1 = 0.1021, wR2 = 0.1347	R1 = 0.0661, wR2 = 0.1370	R1 = 0.2377, wR2 = 0.3060	R1 = 0.2326, wR2 = 0.2583	R1 = 0.3130, wR2 = 0.3435	*R*1 = 0.2087, wR2 = 0.2557

[a] Crystals of the complexes have the following molecular formulas: **1**, {[Mn(3-mbshz)dmso]$_6$·6dmso}; **2**, {[Mn(pashz)dmso]$_6$·4dmso}; **3**, {[Mn(3-dmbshz)dmso]$_6$·6dmso}; **4**, {[Mn$_8$(2-mpshz)$_8$(dmso)$_8$]2·16dmso·5H$_2$O·2MeOH}; **5a**, {[Mn(*RS*-2-mbshz)dmf]$_{10}$·5dmf}; **5b**, {[Mn(*S*-2-mbshz)dmf]$_{10}$·6dmf·2H$_2$O}; **6**, {[Mn(2-dmpshz)py]$_{10}$·5.26dma·4.74py·4H$_2$O}. [b] R1 = $\Sigma||F_o| - |F_c||/\Sigma|F_o|$, wR2 = $[\Sigma w(F_o^2 - F_c^2)^2/\Sigma wF_o^4]^{1/2}$.

Scheme 1. Formation of Hexanuclear, Octanuclear, and Decanuclear Manganese Metalladiazamacrocyles from Ligands Having Different *N*-Acyl Substituents

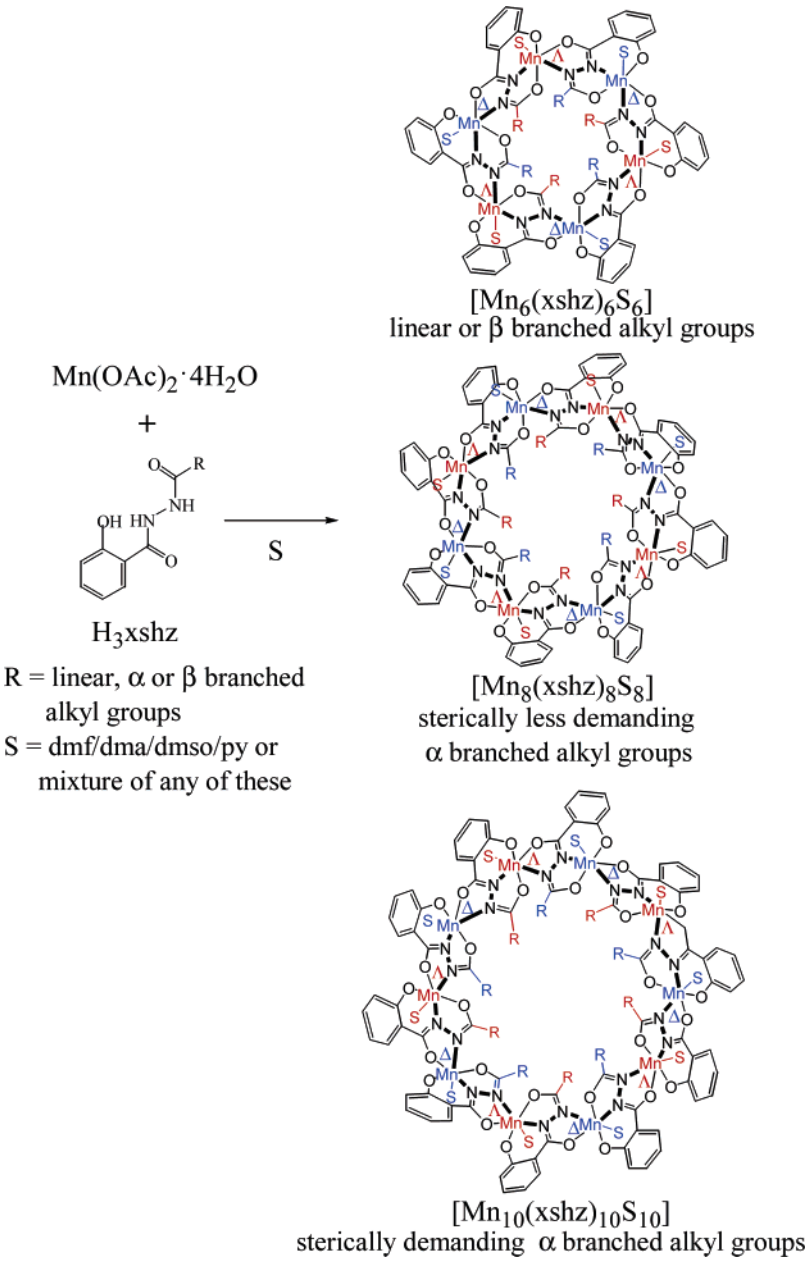

system is decided by the steric and conformational factors of the ligand associated with the ligand−metal assembly. Introduction of different substituents (alkyl/aryl) at the β position of the *N*-acyl group—which is the case with ligands $H_3$3-mbshz, H_3pashz, and $H_3$3-dmbshz—only leads to hexanuclear cyclic systems, as in the ligands with a linear *N*-acyl tail (Scheme 1, top). The system minimizes the steric repulsion between the alkyl/aryl groups at the *N*-acyl tail on its way to cycle formation. In the case of ligands with a β-branched *N*-acyl tail, absence of substituents at Cα facilitates the system in forming a more stable cyclic system with minimum steric repulsion, which is a hexanuclear metallamacrocycle as a natural choice. However, the ligands with sterically demanding α-branched *N*-acyl substituents (H_3*RS*-2-mbshz, H_3*S*-2-mbshz, and $H_3$2-dmpshz) lead to expansion of the macrocyclic ring system (Scheme 1, middle and bottom). Introduction of α-branched *N*-acyl groups results in the formation of a decanuclear metallamacrocycle, where steric interaction of the α-branched *N*-acyl group forces the system into an expanded 30-membered macrocycle during the process of self-assembly (Scheme 1, bottom). However, the same arrangement of ligands for a sterically less demanding α-branched *N*-acyl substituent such as an isopropyl tail ($H_3$2-mpshz) leads to an octanuclear system (Scheme 1, middle), as in a structurally similar iron metallamacrocycle.[10]

Structural Overview of Metallamacrocycles. The macrocycle can be viewed as a ring of Mn ions that is bridged via two intervening hydrazide nitrogen atoms (Scheme 1). All the hexanuclear metallamacrocycles have noncrystallographic S_6 symmetry. The binding mode of the ligand forces the stereochemistry of the metal ions into a propeller configuration. This creates Λ and Δ chiralities at alternate

Chart 2. Schematic Side View of the Core Structures of Hexanuclear and Decanuclear Manganese Metalladiazamacrocycles[a]

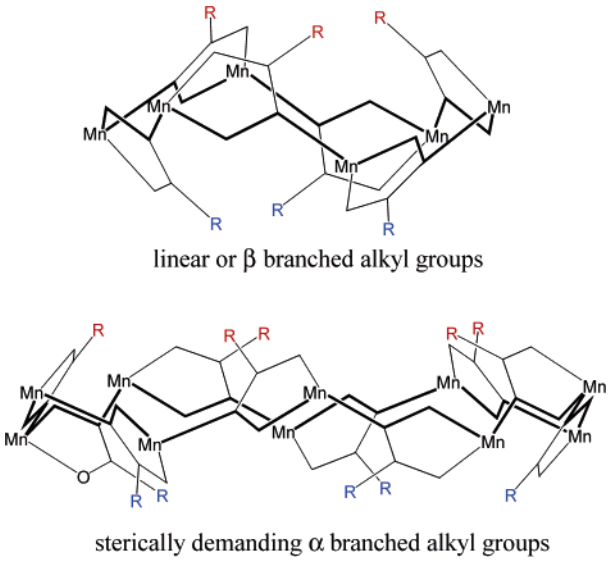

[a] The close contacts are between the next adjacent alkyl/aryl side chains presented in red and blue.

metal centers in the metallamacrocycles (Scheme 1). The hexanuclear metallamacrocycle assumes a cyclohexane-like conformation with respect to the metal ions (Chart 2, top diagram). The cores of all the disc-shaped hexanuclear metallamacrocycles are ~2.1 nm in diameter and ~1.0 nm in thickness. The octanuclear metallamacrocycle of noncrystallographic S_8 symmetry with ~2.3 nm core diameter also adopts a propeller configuration owing to a similar coordination mode of the pentadentate ligand. The alternate occurrence of Λ- and Δ-chirality at the metal center in the metallamacrocycle leads to a cyclooctane-like conformation with respect to the metal ions. Decanuclear metallamacrocycles of noncrystallographic S_{10} symmetry lead to a cyclodecane-like conformation with respect to the metal ions (Chart 2, bottom diagram). The cores of all the disc-shaped decanuclear metallamacrocycles are ~2.6 nm in diameter and ~1.0 nm in thickness. The *N*-acyl substituents of successive ligands are directed alternatively to either face of the metallamacrocycle as a consequence of the stereochemical constraints imposed by the alternate Λ and Δ chiralities at the metal centers (Chart 2). The steric interaction in the metallamacrocycle occurs between the *N*-acyl groups of alternate ligands in the sequential cyclic structure.

Structures of Metalladiazamacrocycles. Structure of [Mn(3-mbshz)(dmso)]$_6$ (1). An ORTEP diagram of **1** is shown in Figure 1a. The complex is in the crystallographic S_6 symmetry site. The overall structure of **1** is very similar to that of other hexanuclear manganese metallamacrocycles (Tables S1 and 2).[8] The local environment of each metal center of high-spin d^4 manganese(III) ion has the same Jahn−Teller elongated octahedral geometry as in other manganese metallamacrocycles. The Jahn−Teller distortion results in elongation of the Mn−N2 and Mn−O4 bond lengths by ~0.3 Å relative to the other Mn−O/N bond lengths. The cyclic structure of the compound leaves a disc-shaped molecule of

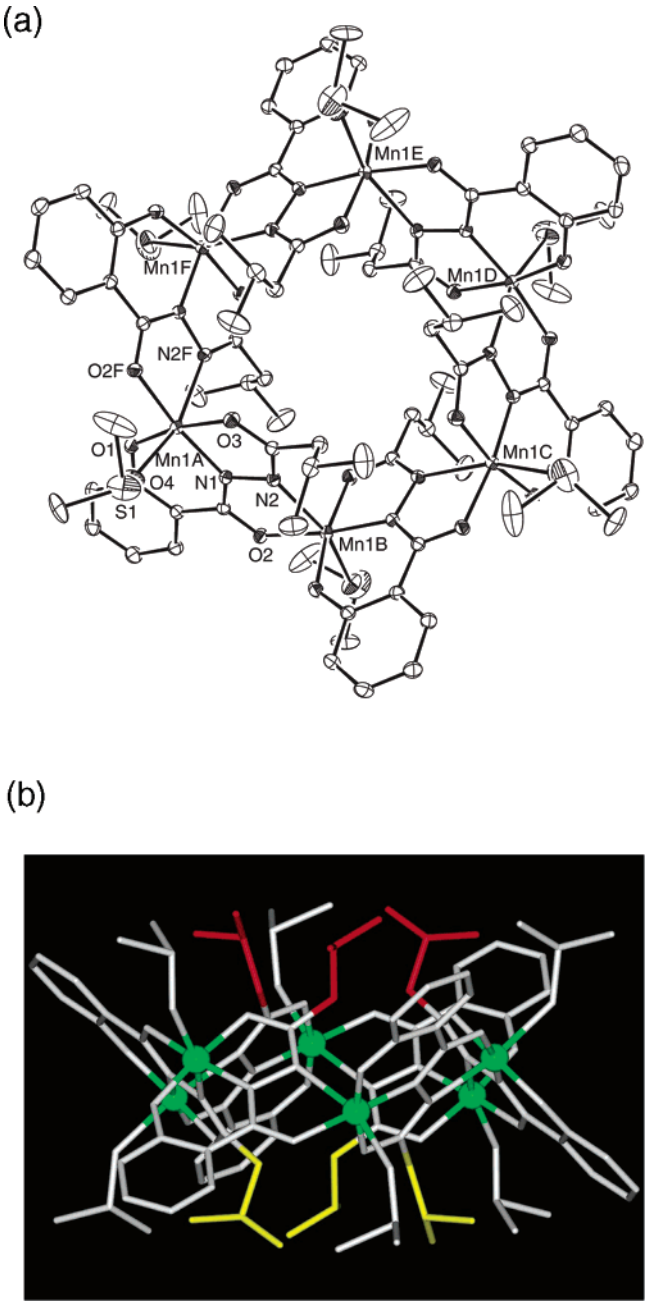

Figure 1. (a) ORTEP diagram of hexanuclear manganese metalladiazamacrocycle **1**. The 18-membered ring was formed from the cyclic −(Mn−N−N)$_n$ linkages. (b) Side view of the disc-shaped metallamacrocycle **1**. Six manganese atoms are represented by green spheres, the alternating three isopropyl side chains in red are shown at one face of the macrocycle, and the remaining three isopropyl side chains in yellow are shown at the opposite face.

nanometer dimensions (Figure 1a,b and Table 2). The molecule has a cavity at its center formed by the *sec*-butyl tails of the ligands (Table 2). The Cα (C9) atoms of the ligand side chains are at closest approach. The *sec*-butyl tails bend away from the cavity entrance to minimize steric repulsion. However, the cavity hole (1.27 Å) is too small to accommodate other guest molecules.

Structure of [Mn(pashz)(dmso)]$_6$ (2) and [Mn(3-dmbshz)(dmso)]$_6$ (3). We attempted to influence the nuclearity of the metallamacrocycles via the steric effect of the ligands, *N*-(phenylacetyl)salicylhydrazide (H_3pashz) and

Table 2. Selected Distances (Å), Angles (deg), and Sizes (Å)[a] for **a**,[b] **1**−**4**, **5a**,**b**, **b**,[c] and **6**

	hexanuclear metallamacrocycles				octanuclear metallamacrocycles		decanuclear metallamacrocycles			
param	**a**	**1**	**2**	**3**	**4**[h]		**5a**	**5b**	**b**	**6**
Mn1A−Mn1B	4.88	4.94	4.89	4.94	4.88	4.90	4.85	4.85	4.95	4.99
Mn1A−M1C	8.18	8.25	8.25	8.26	8.78	8.77	8.84	8.85	9.27	9.30
Mn1A−Mn1B−Mn1C	113.9	113.2	114.4	113.3	127.8	127.2	131.5	131.8	138.9	137.6
close contact[d]	Cα−Cα	Cα−Cα	Cα−Cα	Cα−Cα	Cβ−Cβ	Cβ−Cβ	Cβ−Cβ	Cγ−Cγ, Cβ−Cβ	Cβ−Cγ(Cδ)	Cβ−Cβ
hole size[e]	1.3	1.3	1.3	1.3	2.3	2.2	3.5	3.9,[i] 3.2	4.9	5.3
diameter[f]	20.6	211	20.6	20.7	23.4	23.3	26.5	26.0	26.5	26.8
thickness[g]	11.7	10.7	11.0	11.2	11.4	11.5	12.1	11.8	13.4	11.9

[a] Formulas: **a**, [Mn(hshz)(dmf)]$_6$; **1**, [Mn(3-mbshz)(dmso)]$_6$; **2**, [Mn(pashz)(dmso)]$_6$; **3**, [Mn(3-dmbshz)(dmso)]$_6$; **4**, [Mn(2-mpshz)(dmso)]$_8$; **5a**, [Mn(*RS*−2-mbshz)(dmf)]$_{10}$; **5b**, [Mn(*S*-2-mbshz)(dmf)]$_{10}$; **b**, [Mn(bzshz)(MeOH)]$_{10}$; **6**, [Mn(2-dmpshz)(py)]$_{10}$. [b] [Mn(hshz)(dmf)]$_6$, **a**.[8b] [c] [Mn(bzshz)(MeOH)]$_{10}$, **b**.[11] [d] Atoms of closest approach at the cavity entrance. [e] The hole was formed by the three pseudo-C_3 (**a**, **1**−**3**), the four pseudo-C_4 (**4**), and the five pseudo-C_5 (**5a**,**b**, **b**, and **6**) symmetry-related nearest selective atoms toward the ring center, and the size of the hole was calculated by subtracting the van der Waals radii of the constituting atoms. [f] Diameter of the metalladiazamacrocycle was calculated from the distance between the three pseudo-C_3 (**a**, **1**−**3**) and the five pseudo-C_5 (**5a**,**b**, **b**, and **6**) symmetry-related phenyl hydrogen atoms of the ligand, where the van der Waals radius of the hydrogen atom was assumed to be 1.10 Å. [g] Thickness of metallamacrocycle. [h] The compound **4** contains two chemically similar but crystallographically independent molecules. [i] **5b** has two different hole sizes because of two different diastereomeric cavity environments on either face of the metallamacrocycle.

N-(3,3-dimethylbutanoyl)salicylhydrazide ($H_3$3-dmbshz), which have slightly bulkier substituents at the β position of the *N*-acyl side chain. However, both ligands, pashz^{3-} and 3-dmbshz^{3-}, also produced hexanuclear manganese metallamacrocycles [Mn(pashz)(dmso)]$_6$ (**2**) and [Mn(3-dmbshz)(dmso)]$_6$ (**3**). Ball and stick diagrams of **2** are shown in Figure 2. Both **2** and **3** have noncrystallographic S_6 symmetry. Although terminal acyl groups of the ligands are bulkier than the *sec*-butyl tail, the flexibility of the Cβ carbon again leads to formation of a hexanuclear metallamacrocycle. Metallamacrocycles **2** and **3** are also structurally very similar to other hexanuclear manganese metallamacrocycles (Tables S1 and 2). Overall dimensions of the metallamacrocycles are comparable to those of other hexanuclear manganese metallamacrocycles.[7b,8,9a]

Structure of [Mn(2-mpshz)(dmso)]$_8$ (4). In this case we attempted to affect the ring size and geometrical features of the metallamacrocycles by a simple shift of the branched methyl group at the β position of the *sec*-butyl tail of the ligand to the α position. The shift has expanded the ring size of the metallamacrocycles, from a hexanuclear to an octanuclear system. Ball and stick diagrams of **4** are shown in Figure 3. Metallamacrocycle **4** with noncrystallographic S_8 symmetry is at the crystallographic general position. The steric interaction between methyl substituents at the Cα position of the *N*-2-methylpropanoyl group might have caused the ring expansion from an 18-membered to a 24-membered ring system.

Structures of [Mn(*RS*-2-mbshz)(dmf)]$_{10}$ (5a) and [Mn(*S*-2-mbshz)(dmf)]$_{10}$ (5b). We also attempted to affect the ring size and geometrical features of the metallamacrocycles by changing two factors, the steric interaction and the chirality of the ligand. In line with this strategy, we used the sterically demanding and chiral α-branched *N*-acyl ligands, H_3*RS*-2-mbshz and H_3*S*-2-mbshz. The introduction of a sterically demanding α-branched *N*-acyl group has further expanded the ring size of the metallamacrocycles, from an octanuclear to a decanuclear system. Ball and stick diagrams of **5a** are shown in Figure 4. **5a** has noncrystallographic S_{10} symmetry and is at the crystallographic inversion center. The steric interaction between alkyl substituents at the Cα position of the *N*-(*R*,*S*)-2-methylbutanoyl

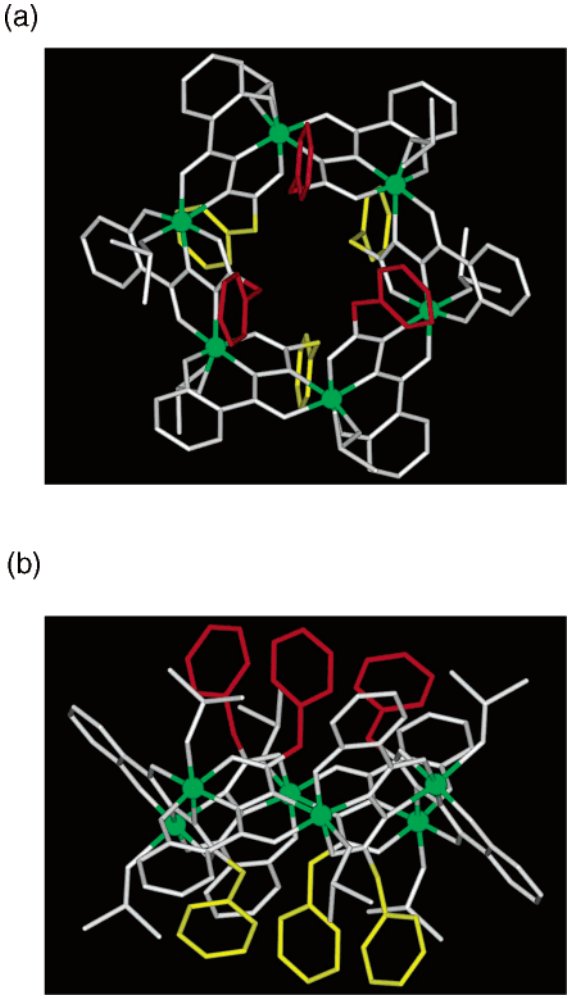

Figure 2. Ball and stick diagram of hexanuclear manganese metalladiazamacrocycle **2**: (a) top view; (b) side view. Manganese atoms are represented by green spheres, and the benzyl side chains are represented in red and yellow.

group has caused ring expansion from a 24-membered to a 30-membered ring system. The racemic *N*-(*R*,*S*)-2-methylbutanoyl group directed into the cavity of the metallamacrocycle shows the alternate *R*, *S* chiral configuration. Complexation of the same but enantiopure H_3*S*-2-mbshz leads to another dodecanuclear metallamacrocycle but with no inversion symmetry. **5b** is in the crystallographic inversion

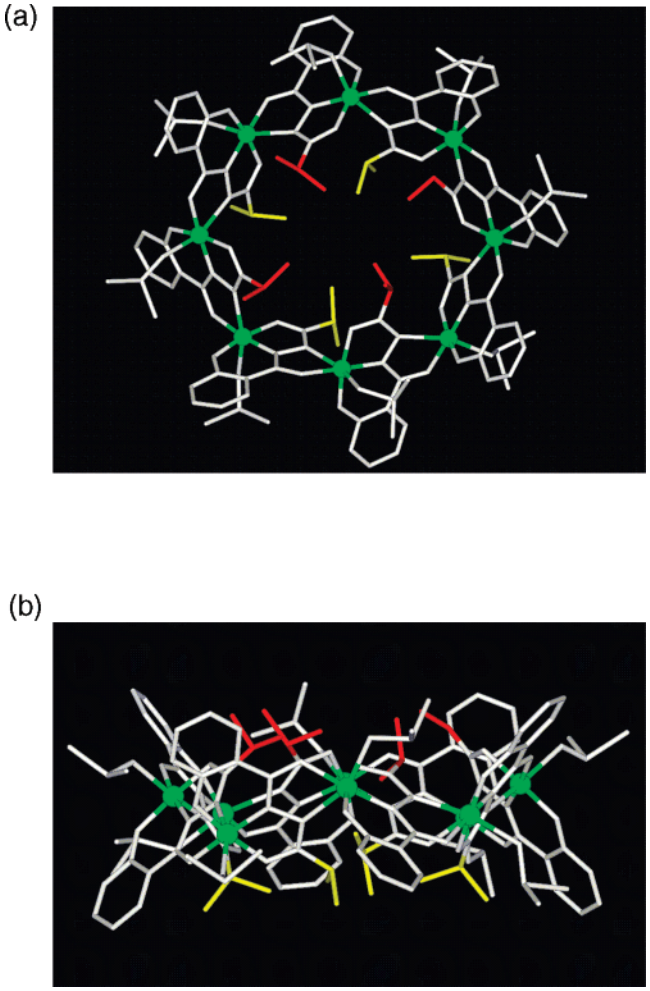

Figure 3. Ball and stick diagram of octanuclear manganese metalladiazamacrocycle **4**: (a) top view; (b) side view. Manganese atoms are represented by green spheres, and the isopropyl side chains are represented in red and yellow.

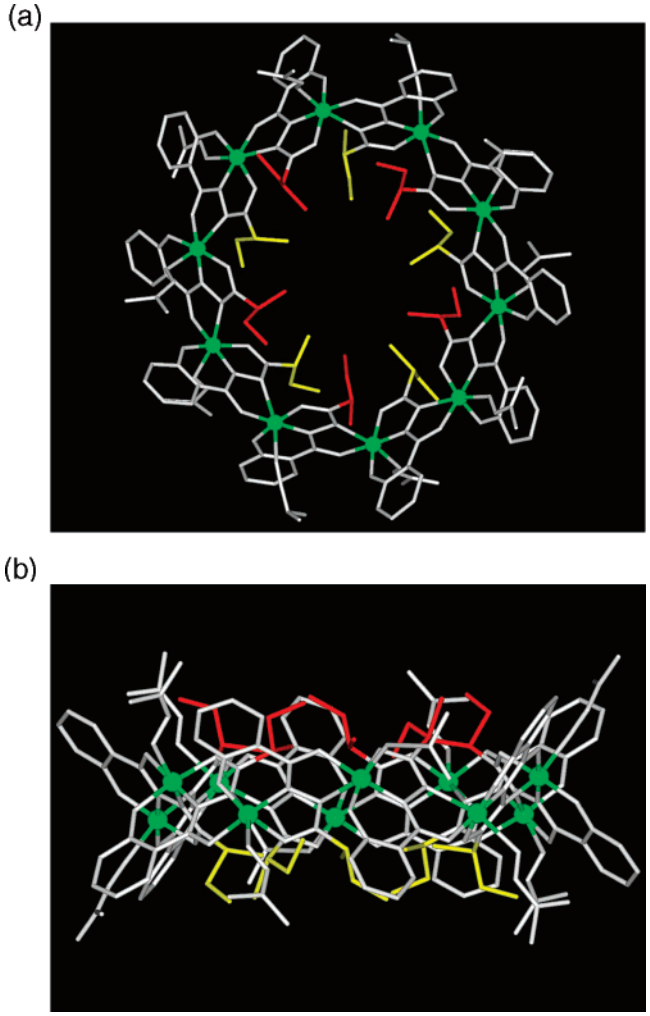

Figure 4. Ball and stick diagram of decanuclear manganese metalladiazamacrocycle **5a**: (a) top view; (b) side view. Manganese atoms are represented by green spheres, and the *sec*-butyl side chains are represented in red and yellow.

center and is statistically disordered. All geometric parameters of **5b** are similar to those of **5a** except for the environment of the cavity. While both faces of **5a** have the same cavity environment, **5b** with the enantiopure H_3*S*-2-mbshz ligand has two slightly different diastereomeric cavity environments that result from the *N*-acyl substituents of the same chirality but with metal centers of different stereochemistry. The sizes of the cavity entrances on either side of **5b** differ (Table 2).

Structure of [Mn(2-dmpshz)(py)]$_{10}$ (6). In another attempt to influence the ring size, we used a ligand with two alkyl substituents at the Cα position, *N*-(2,2-dimethylpropanoyl)salicylhydrazide ($H_3$2-dmpshz). Crystals of complex **6** could be isolated from a mixed solvent, dma/pyridine in the ratio of 3:1. The crystals contain both pyridine and dma molecules as solvent. However, only pyridine is coordinated to the metal center. Ball and stick diagrams of **6** are shown in Figure 5. Compound **6**, of noncrystallographic S_{10} symmetry, is in the crystallographic inversion center. Although the sterically more demanding 2,2-dimethylpropionyl side chain was introduced as *N*-acyl substituent, the system still preferred a decanuclear metallamacrocycle. However, the sterically more demanding *tert*-butyl group of the ligand increased the hole size of **6** (5.3 Å) compared with **5a** (3.5 Å) and **5b** (3.9, 3.2 Å).

Comparison of Metalladiazamacrocycles. Our strategy for the modulation of the metallamacrocycles was to modify the steric factors of the *N*-acyl side chains of the ligands to control the size and nuclearity of the corresponding metallamacrocycles.

All hexanuclear manganese metalladiazamacrocycles with β-branched *N*-acyl substituents used have not only the same overall structures but also the same local environment (Tables S1 and 2). The bond distances and angles around the metal centers vary marginally from one to the other. The distances between the neighboring metal centers (Mn1A···Mn1B, 4.88−4.94 Å) and the near neighboring metal centers (Mn1A···Mn1C, 8.18−8.26 Å) are in a narrow range. The Mn−Mn−Mn angles around three consecutive metal centers (113.2−114.4°) are also in a narrow range and close to the value of the ideal geometry of cyclohexane (114.4°). The β-substitution does not induce any ring expansion of the metallamacrocycles nor significant structural modifications. The presence of a methyl group at the β position of the *N*-acyl group in (3-methylbutyryl)salicylhydrazidate is not

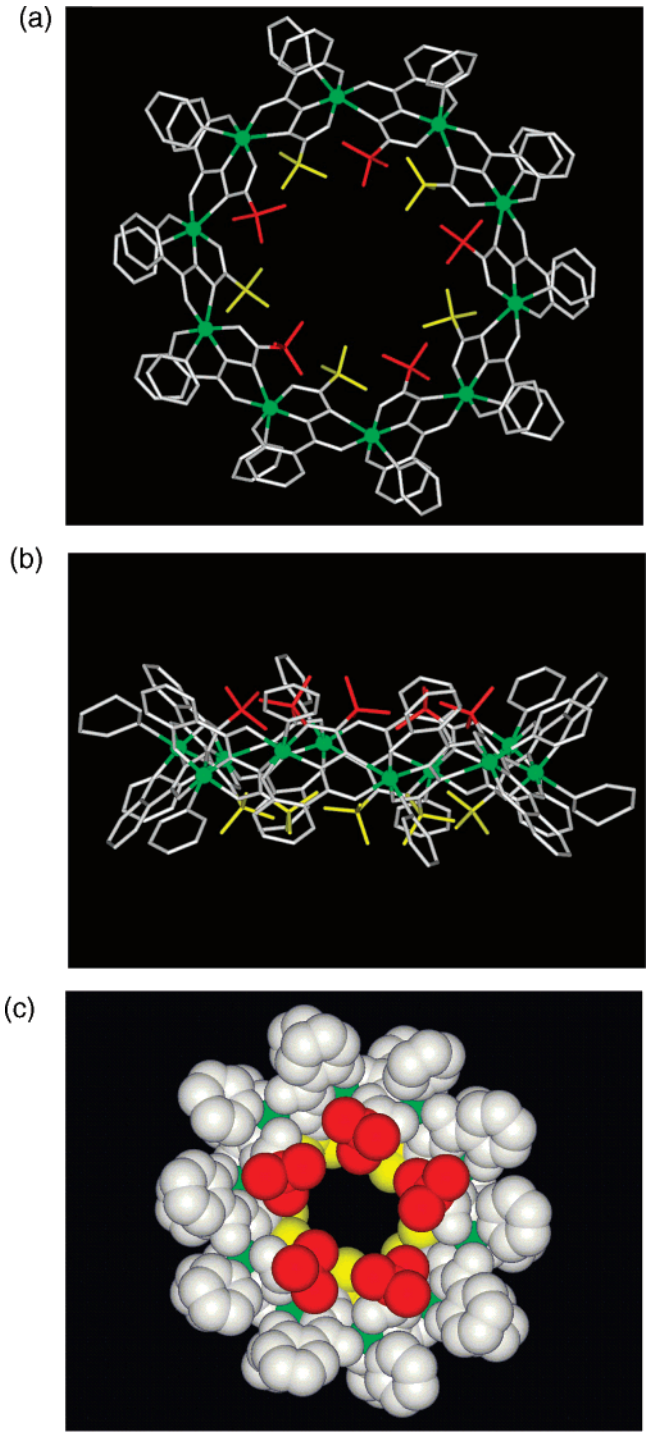

Figure 5. (a) Ball and stick diagram of decanuclear manganese metalladiazamacrocycle **6**: top view; (b) side view. (c) Space-filling diagram of **6** with a cavity in the center of the macrocycle. Manganese atoms are represented by green spheres, and the *tert*-butyl side chains are represented in red and yellow.

sufficient to cause expansion of the macrocycle into a higher member because the flexibility at the β carbon atom favors a suitable ordering of the methyl group. The salicylhydrazide ligands with benzyl or *tert*-butyl groups at the *N*-acyl position also lead to hexanuclear metalladiazamacrocycles with the same stoichiometry, which indicates, contrary to our expectation, that a bulkier group at the β position has no influence in expanding the ring to the next higher number. This could be because the steric repulsion between the β substituents could be minimized by free rotation about the Cα−Cβ bond.

The introduction of α substituents not only leads to expansion of the metallamacrocycle ring system from hexanuclear to octanuclear or decanuclear but also accompanies the structural modifications in overall and local geometries. While the bond distances around the metal center were not affected, some of the bond angles were affected by the ring expansion. The bond distances around the metal center are similar, irrespective of the nuclearity of the metallamacrocycles and variation in the *N*-acyl substituents of the ligands. However, some bond angles around the metal centers, the metal−metal distances, and Mn−Mn−Mn angles are affected by the variation in *N*-acyl substituents (Tables S1 and 2). The key geometrical features affected are the N1−Mn1−N2 bond angles, which are related to the overall metalladiazamacrocyclic ring structures. The bond angles increase as the metallamacrocycles expand from a hexanuclear to a decanuclear system. The average bond angle of 102.6° in hexanuclear structures has increased to 110.9° in decanuclear structures. The higher steric repulsion of *N*-acyl substituents causes the larger N1−Mn1−N2 bond angles. Within the hexanuclear system, the variation of the bond angles (101.8−103.4°) is not manifest. However, the additional variation of the bond angles (106.8, 106.9° for **5a**,**b**; 114.9, 115.0° for **b** ([Mn(bzshz)(MeOH)]$_{10}$, where bzshz is *N*-benzoylsalicylhydrazidate),[11] **6**) can be seen within the decanuclear system. Surprisingly, the bond angles of 107.4 and 106.9° in the octanuclear structures are rather similar to those in decanuclear **5a**,**b** (106.8, 106.9°). The strain caused by the ring expansion propagates to other bond angles around the metal centers. The O1−Mn−N2 bond angle is also affected by the ring expansion of the metallamacrocycles from the hexanuclear to the decanuclear system (Table S1). The average bond angle for O1−Mn−N2, 95° in the hexanuclear structure, has decreased to 91° in the octanuclear and 90° in the decanuclear structure. These variations of the bond angles around the metal centers are reflected in the overall geometries of the metallamacrocycles. Although the distances between neighboring metal centers are similar (Table 2), the distances between the near neighboring metal centers in the decanuclear structures (Mn1A···Mn1C, 8.84−9.30 Å) are ∼1 Å longer than those in the hexanuclear structures (Mn1A···Mn1C, 8.18−8.26 Å). Again, the additional variation in the angles (106.8, 106.9° for **5a**,**b**; 114.9, 115.0° for **b**, **6**) can be seen within the decanuclear system. A similar relationship between the octanuclear structure **4** and decanuclear structures **5a**,**b** could be observed in the distance between the next adjacent metal centers as in the bond angle around the metal center, N1−Mn1−N2. The distances in the decanuclear **5a**,**b** (8.84, 8.85 Å) are closer to those in the octanuclear structures (8.78, 8.77 Å) than to those in decanuclear **b** and **6** (9.27, 9.30 Å). The most significant difference is observed in the Mn1A−Mn1B−Mn1C angles around three consecutive metal centers. The values in the decanuclear structures (131.5−138.9°) are ∼20° larger than those in the hexanuclear

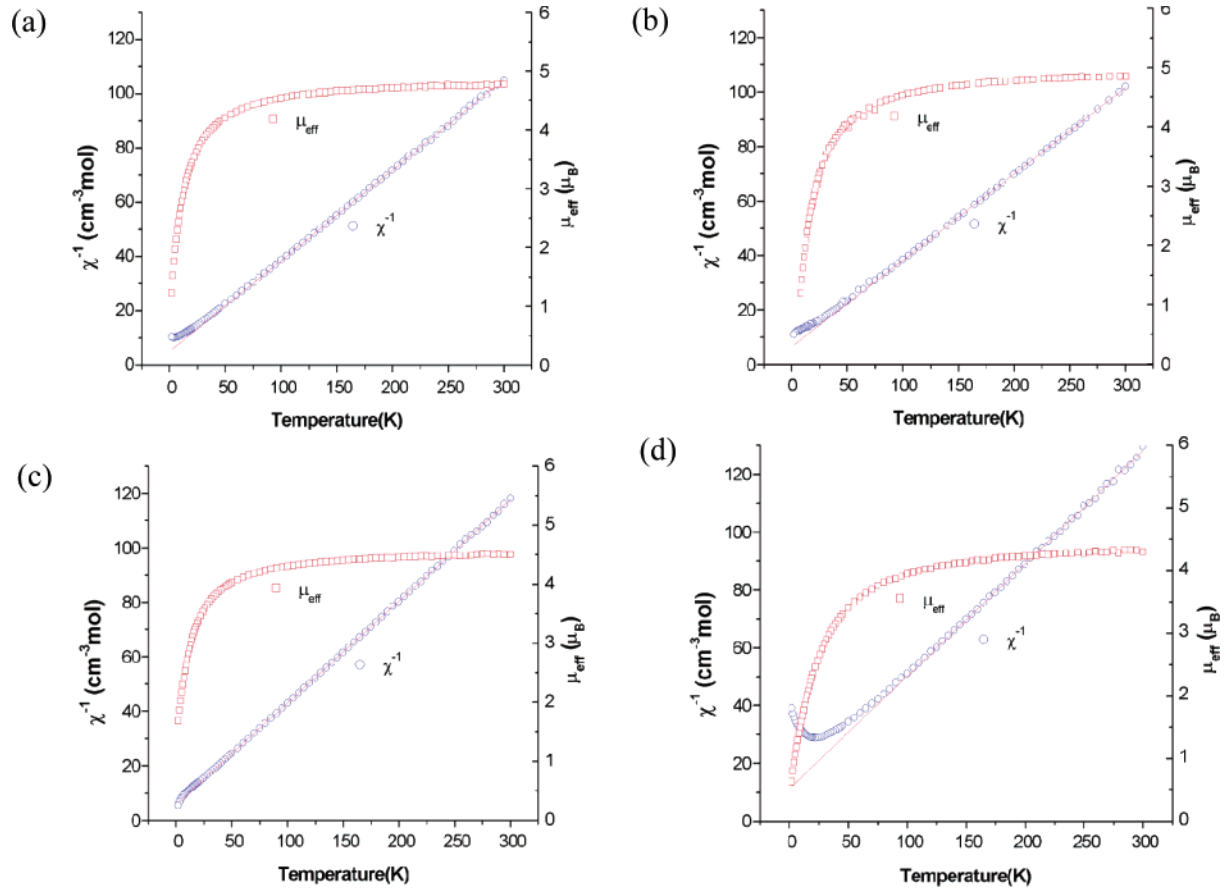

Figure 6. Plots of the effective magnetic moment (μ_{eff}) and the inverse magnetic susceptibility (χ^{-1}) as a function of temperature for compounds (a) **2**, (b) **3**, (c) **5a**, and (d) **6**. Note that the unit of μ_{eff} is μ_B/Mn ion and the unit of the magnetic susceptibility is cm^3/mol of Mn ion.

structures (113.2−114.4°). A similar relationship between octanuclear structure **4** and decanuclear structures **5a**,**b** could also be observed. The local geometries of decanuclear **5a**,**b** are rather similar to those of octanuclear structure **4** rather than the other decanuclear structures, **b** and **6**. The entrance to the cavities at the center of the hexanuclear metallamacrocycles is composed of the Cα carbons of the *N*-acyl substituents. With sterically less demanding linear or *β*-branched *N*-acyl substituents, the close contacts in the hexanuclear structures occur between the unbranched Cα carbons of the near neighboring ligands. In the hexanuclear metallamacrocycles the distance between Cα carbon atoms is ∼4 Å, whereas it increases to ∼6 Å in octanuclear and decanuclear metallamacrocycles to accommodate the increased steric interaction, leading to expansion of the ring size. The close contacts in octanuclear and decanuclear structures occur between the C*β*−C*β*, C*γ*−C*γ*, and C*β*−C*δ* carbons of the adjacent ligands. The overall dimensions of the metallamacrocycles increase as expected from 20.6 to 21.1 Å in diameter and 10.7−11.7 Å in thickness for hexanuclear structures to 23.3−23.4 Å in diameter and 11.4−11.5 Å in thickness for octanuclear structures, and 26.0−26.8 Å in diameter and 11.8−13.4 Å in thickness for decanuclear structures. The increase in diameter of the metallamacrocycles reflects the increase in the ring size from 18-membered to 24- and 30-membered ring systems. However, the thickness rather reflects the length and size of the *N*-acyl substituents. Details of the structural modifications are listed in Table 2.

Magnetic Properties. Figure 6 shows plots of the temperature dependence of the effective magnetic moment (μ_{eff}) and the inverse magnetic susceptibility (χ^{-1}) of the complexes **2**, **3**, **5a**, and **6** for the temperature range 2−300 K. The magnetic properties of all the metallamacrocycles show a similarity in behavior, whereby μ_{eff}/Mn ion slightly decreases with decreasing temperature and below ∼50 K decreases rapidly. This behavior is typical for weakly coupled antiferromagnetic systems. Thus, by fitting the magnetic susceptibility data at high temperatures $T > 60$ K to the Curie−Weiss expression $\chi^{-1}(T) = C/[T + \Theta]$, we obtained an effective coupling constant J_{eff} and an effective magnetic moment per metal ion μ_{eff} for each metallamacrocycle, the fitting results being summarized in Table 3.

The obtained values of $\mu_{eff} = 4.5-5.0\ \mu_B$ are in excellent agreement with $g[S(S+1)]^{1/2} = 4.90\ \mu_B$, the value for an uncorrelated paramagnetic spin with $S = 2$. The small and negative values of $J_{eff} = -8.5$ to -3.8 K indicate that these metallamacrocycles are weakly coupled antiferromagnetic systems. In this kind of cyclic system, only the exchange interactions between the neighboring centers (J_1) and between the next-neighboring centers (J_2) are usually taken into account, since the distances between the paramagnetic centers in other positions are greater than ∼8 Å. Thus, $J_{eff} = J_1 +$

Table 3. Effective Magnetic Moments and Coupling Constants for **a**,[a] **2**, **3**, **5a**, **b**,[b] and **6**

	hexanuclear metallamacrocycles			decanuclear metallamacrocycles		
param	**a**	**2**	**3**	**5a**	**b**	**6**
J_{eff}[c] (K)	−4.33	−3.84	−4.88	−4.40	−1.275, −0.73[d]	−8.49
μ_{eff}[e] (μ_B)	4.9	4.9	5.0	4.6	4.7	4.5

[a] Unpublished result for $[Mn(hshz)(dmf)]_6$ (**a**). [b] $[Mn(bzshz)(MeOH)]_{10}$ (**b**).[11] [c] The J_{eff} values (expressed in K) are between the adjacent manganese centers for **a**, **2**, **3**, **5a**, and **6**. [d] Referring to the values $J_1 = J_{AB} = -1.275$ K and $J_2 = J_{AC} = -0.73$ K for the compound **b** from ref 11, $J_{eff} = J_1 + J_2 = -2.0$ K for compound **b** and is comparable to the values we obtained here. [e] The effective magnetic moments are calculated per metal ion.

J_2 because the number of neighbors is 2 and is the same for both J_1 and J_2 in this cyclic system.

Conclusion

We have accomplished the synthesis of seven different manganese metalladiazamacrocycles by modification of the *N*-acyl side chain of the ligand. Substitution at the Cβ position of the *N*-acyl side chain resulted in 18-membered hexanuclear systems, while the introduction of Cα substituents caused the expansion of the ring to yield 24-membered octanuclear or 30-membered decanuclear systems, depending on the size of the substituents introduced. The hexanuclear systems generated by Cβ branched *N*-acylsalicylhydrazide ligands had structural features similar to those of the unbranched (linear) *N*-acyl ligand. Close contact occurs between the Cα carbons of the *N*-acyl side chain, so the size of the Cβ substituents used in this study has only a marginal influence on the geometrical features of hexanuclear structures. The introduction of the Cα substituents not only changes the nuclearity of the metallamacrocycles but also influences the local features of metallamacrocycles. Close contact occurs between the Cβ, Cγ, and Cδ carbons; in other words, it does not occur between the Cα carbons. The ligand with the sterically least demanding Cα substituent, $H_3$2-mpshz, leads to formation of an octanuclear metallamacrocycle, **4**. The Cα substituent expanded the nuclearity of the metallamacrocycle from six to eight. The angles related to the ring formation in the octanuclear structure are more strained than those in the hexanuclear structures. Ligands with sterically more demanding Cα substituents, H_3*RS*-2-mbshz and H_3*S*-2-mbshz, further expanded the macrocyclic ring system to 30-membered decanuclear metallamacrocycles, **5a**,**b**. Even though the nuclearity of **5a**,**b** is 10, the local environment of the ring metal center is similar to that of octanuclear metallamacrocycle **4**. This observation suggests that the strain related to the formation of the macrocycles in decanuclear **5a**,**b** is similar to that in octanuclear **4**. The ligand with the sterically most demanding Cα substituent, $H_3$2-dmpshz, results in the same 30-membered decanuclear metallamacrocycle, **6**, but the local environments related to the ring formation are more strained than in **5a**,**b**. We have observed that the nuclearity of the metallamacrocycles and geometric features such as the Mn−Mn−Mn angle, close contacts between the *N*-acyl side chains, and cavity sizes can be tuned by careful and systematic modification of the ligand *N*-acyl group. The size and shape of the substituents influence the nuclearity and the features of metalladiazamacrocycles because close contacts are occurring between the *N*-acyl substituents. This work gives a better insight into the engineering aspect of metalladiazamacrocycles.

Acknowledgment. The authors wish to acknowledge the financial support of KISTEP (Grant M1-0213-03-0004), Hanyang University (Grant HY 2004-1), and CBMH. B.J.S. also acknowledges the support of Korean Science and Engineering Foundation (KOSEF) grant (R01-2003-000-10849-0).

Supporting Information Available: An X-ray crystallographic file in CIF format for the structure determination and a table for selected bond lengths and angles of the metallamacrocycles (Table S1). This material is available free of charge via the Internet at http://pubs.acs.org.

IC050891H